

# Combined effects of Li content and sintering temperature on polymorphic phase boundary and electrical properties of Li/Ta co-doped (Na, K)NbO<sub>3</sub> lead-free piezoceramics

Zong-Yang Shen · Ke Wang · Jing-Feng Li

Received: 23 March 2009 / Accepted: 21 July 2009 / Published online: 31 July 2009  
© Springer-Verlag 2009

**Abstract** Crystallographic structure, phase transition and electrical properties of lead-free  $(\text{Na}_{0.535}\text{K}_{0.485})_{1-x}\text{Li}_x(\text{Nb}_{0.942}\text{Ta}_{0.058})\text{O}_3$  ( $x = 0.042\text{--}0.098$ ) ( $\text{NKL}_x\text{NT}$ ) piezoelectric ceramics were investigated. The experimental results show that both Li content and sintering temperature strongly affect the orthorhombic–tetragonal polymorphic phase boundary (PPB), which results in remarkable differences of the piezoelectric property and its temperature stability in the  $\text{NKL}_x\text{NT}$  ceramics. Chemical analysis indicates that sodium volatilizes more seriously than potassium and lithium with increasing sintering temperature. Due to the comprehensively optimized effects of Li content and sintering temperature, an enhanced piezoelectric constant  $d_{33}$  (276 pC/N) was obtained at room temperature in the ceramics with  $x = 0.074$  sintered at 1000°C. In the same composition, a further high  $d_{33}$  up to 354 pC/N was obtained at 43°C, which is close to its  $T_{0-t}$  temperature. Furthermore, better temperature stability can be obtained when  $x = 0.082$  sintered at 1000°C, whose piezoelectric constant  $d_{33}$  (236 pC/N) keeps almost constant from room temperature to 100°C. Such a temperature-independent piezoelectric property is available in the  $\text{NKL}_x\text{NT}$  ceramics with high Li content because its  $T_{0-t}$  was moved below room temperature.

**PACS** 77.84.Dy · 77.80.Bh · 77.65.Bn · 77.22.Ch · 61.05.cp

Z.-Y. Shen · K. Wang · J.-F. Li (✉)  
Department of Materials Science and Engineering, State Key Laboratory of New Ceramics and Fine Processing, Tsinghua University, Beijing 100084, People's Republic of China  
e-mail: [jingfeng@mail.tsinghua.edu.cn](mailto:jingfeng@mail.tsinghua.edu.cn)

## 1 Introduction

Conventional lead-based piezoelectric ceramics such as  $\text{Pb}(\text{Zr}_x\text{Ti}_{1-x})\text{O}_3$  (PZT) are widely used in sensors and actuators due to their excellent piezoelectric properties [1]. However, because of high toxicity of Pb element, environmental and safety concerns with respect to the utilization, recycling, and disposal of lead-based piezoelectric ceramics have induced a new surge in developing lead-free piezoelectric ceramics [2–9].

Recently, much attention for lead-free piezoelectric ceramics has mainly focused on (Na, K)NbO<sub>3</sub> (NKN)-based ceramics because the excellent piezoelectric properties are discovered in textured Li-, Ta-, and Sb-modified (Na,K)NbO<sub>3</sub> ceramics by Y. Saito et al. [2]. In NKN-based ceramics, recent studies revealed that the orthorhombic–tetragonal polymorphic phase boundary (PPB) strongly affects its piezoelectric properties [8, 9], and a coexistence of the orthorhombic and tetragonal phases, i.e. a PPB, near room temperature, rather than the formation of the morphotropic phase boundary (MPB) similar to that observed in the PZT system [10], would be helpful to obtain enhanced piezoelectric properties. Meanwhile, according to previous work [9], although high  $d_{33}$  value can be obtained using Sb ion on the pentavalent sites of the perovskite lattice, it is preferable to avoid the use of toxic Sb element for health and environmental reasons. Therefore, the piezoelectric properties of Li- and Ta-modified NKN ceramics are themselves sufficient to arouse keen interest in further developing alkali niobate tantalates as a viable lead-free alternative piezoelectric ceramics.

Among reported Li- and Ta-modified NKN ceramics, owing to the shift of the  $T_{0-t}$  to near-room temperature, the enhancement of piezoelectric properties can be obtained [11].

However, associated with a PPB, an issue of property instability against temperature increases the difficulty for applications [8]. Besides this issue, there are also several points of limitations existing. Firstly, these ceramics contain a large amount of Ta element ( $\geq 10$  mol%), and adding large amounts of Ta to NKN ceramics will limit the applications of these materials because the price of  $Ta_2O_5$  is much more high than that of  $Nb_2O_5$ . Secondly, in order to improve stability, while maintaining high piezoelectric properties, it is desirable to shift the  $T_{o-t}$  out of the application temperature range (usually  $-50$ – $200^\circ C$ ), but unfortunately, in Li- and Ta-modified NKN ceramics as usual, further shifting of the  $T_{o-t}$  downward below room temperature cannot be achieved owing to solubility limitations (6–8%), where excessive additions lead to undesirable second phases, thus deteriorating their properties [12]. Finally, the sintering temperature of these ceramics is usually higher than  $1070^\circ C$ , and this high sintering temperature accelerates the volatilization of  $Na_2O$  [13], so that impurity phase such as  $K_3Li_2Nb_5O_{15}$  [12], which prevents parts of Li from entering the perovskite lattice, can be more easily formed. Actually, low sintering temperature is favorable for increasing Li doping amount, and this is confirmed by our recent work [14].

In this work, we prepared Li- and Ta-modified NKN lead-free ceramics, i.e.  $(Na_{0.535}K_{0.485})_{1-x}Li_x(Nb_{0.942}Ta_{0.058})O_3$  ( $NKL_xNT$ ), by the conventional solid-state sintering method, where no undesirable second phases are observed even for Li doping amount up to 0.098. In the  $NKL_xNT$  ceramics with Li content  $x = 0.082$  sintered at  $1000^\circ C$ , because its  $T_{o-t}$  temperature is moved below room temperature, we obtained a relatively high piezoelectric constant  $d_{33}$  (236 pC/N), which is nearly temperature-independent from room temperature to  $100^\circ C$ . It should be noted here that the Ta content is fixed at 0.058 because a small amounts of Ta are beneficial to improve sintering behavior and cannot increase the sintering temperature excessively. Meanwhile, through optimizing the added amounts of sodium and potassium, Na:K ratio is fixed at 0.535:0.485. Our investigations of this study are mainly focused on the combined effects of Li content and sintering temperature on the crystallographic structure, phase transition and electrical properties of  $NKL_xNT$  ceramics.

## 2 Experimental

$(Na_{0.535}K_{0.485})_{1-x}Li_x(Nb_{0.942}Ta_{0.058})O_3$  ceramics, where  $x = 0.042$ – $0.098$ , were prepared by a conventional ceramic fabrication method using reagent grade  $Na_2CO_3$ ,  $K_2CO_3$ ,  $Li_2CO_3$ ,  $Nb_2O_5$ , and  $Ta_2O_5$  as starting materials. For each composition, the starting materials were weighed according to the stoichiometric formula and ball milled for 24 h in ethanol using  $ZrO_2$  balls. After separating the balls, the slurries were dried and calcined at  $750^\circ C$  for 5 h, and then ball

milled again for 24 h and dried. Without any special treatment, the powders were subsequently pre-pressed to pellets 15 mm in diameter, followed by a cold isostatic pressing (CIP) under 200 MPa. Using a heating rate of  $10^\circ C/min$ , sintering was carried out at  $980$ – $1060^\circ C$  for 2 h in air. Bulk densities of sintered pellets were measured using the Archimedes method. X-ray diffraction (XRD) characterization of the ceramics was performed using  $Cu K\alpha_1$  radiation ( $\lambda = 1.5406 \text{ \AA}$ ) filter through Ni foil. Inductively Coupled Plasma (ICP) method was used to detect sodium, potassium and lithium contents in the final ceramic bodies, and the distribution of chemical elements in microscale regions were analyzed using Energy Dispersive Spectrometer (EDS) after the sample surfaces were polished to a mirror-like face.

For electrical characterization, ceramic samples were polished and painted with silver paste on both sides. Dielectric constants at 100 kHz of the ceramics were measured as a function of temperature using an Agilent 4294A precision impedance analyzer. For piezoelectric and electromechanical measurements, the ceramic samples were poled at  $120^\circ C$  for 30 min under an electric field of 3 kV/mm in silicone oil. The piezoelectric constant  $d_{33}$  was measured using a quasi-static piezoelectric constant testing meter (ZJ-3A, Institute of Acoustics, Chinese Academy of Science, Beijing, China). The planar mode electromechanical coupling factor  $k_p$  was determined by a resonance and antiresonance methods performed on the basis of IEEE standards using an impedance analyzer (Agilent 4294A). The polarization–electric field ( $P-E$ ) hysteresis loop was measured by a Radian Precision workstation based on a standard Sawyer–Tower circuit at room temperature.

## 3 Results and discussion

Figure 1 shows the bulk densities of the  $NKL_xNT$  ceramics with  $x = 0.042$ ,  $0.066$ ,  $0.074$  and  $0.090$  sintered at different temperatures. Ranging over different  $x$  values in the  $NKL_xNT$  ceramics (some compositions are not shown in Fig. 1), the sintering temperatures corresponding to the highest bulk density are  $1040^\circ C$ ,  $1000^\circ C$  and  $980^\circ C$ , respectively for the Li contents  $x = 0.042$ ,  $x = 0.050$ – $0.082$  and  $x = 0.090$ – $0.098$ . High Li content  $x$  is in favor of obtaining the highest bulk density at low sintering temperatures. Actually,  $Li_2O$  itself is a good sintering aid on the purpose of reducing sintering temperature for the preparation of piezoelectric ceramics [15, 16]. For each composition, the bulk density, after reaching the peak value, decreases gradually with increasing sintering temperature owing to the volatilization of alkali metal ions [17].

Figure 2a shows the XRD patterns of the  $NKL_xNT$  ceramics with  $x = 0.074$  sintered at  $980$ – $1040^\circ C$ . The enlarged XRD patterns of the ceramics in the ranges of  $2\theta$

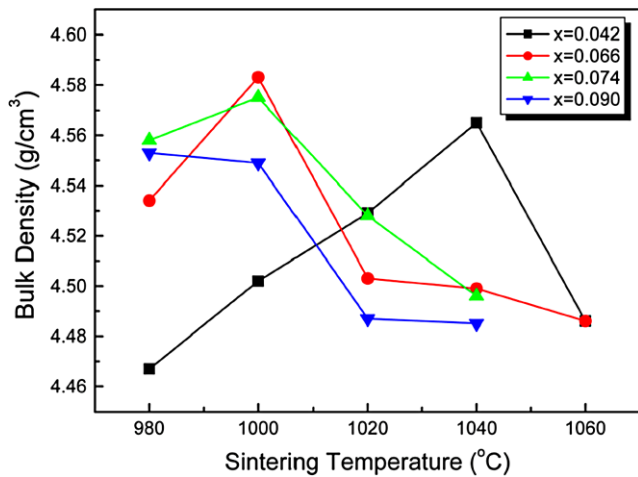
from 30° to 33° and from 44° to 47° are shown in Fig. 2b and c, respectively. As shown in Fig. 2b, only one peak can be seen when the ceramics were sintered at 980–1000°C, while a shoulder peak is attached onto its right side when sintered above 1020°C. Meanwhile, according to Fig. 2c, when the sintering temperature exceeds 1020°C, the (002) and (200) peaks apparently split. All these characteristics demonstrate the coexistence of orthorhombic and tetragonal phases in the ceramics sintered at 980–1000°C, while the tetragonal phase becomes dominant when sintered above 1020°C. In our previous studies [13, 18], this kind of temperature dependence of phase structure transition behavior was also found, and we attributed it to the different extents of the volatilization of alkali metal ions during sintering at different temperatures. In this study, we detected sodium, potassium and lithium contents of the  $\text{NKL}_x\text{NT}$  ceramics

with  $x = 0.074$  sintered at 980–1060°C using ICP method. The results of chemical analysis are shown in Table 1.

As can be seen from Table 1, when the sintering temperature is 980°C, the volatilization of alkali metal ions is slight compared with calculated values according to the stoichiometric composition. However, when the sintering temperature was over 1000°C, extents of the volatilization of alkali metal ions different from the results listed in Table 1 are observed. Especially, with increasing sintering temperature, sodium volatilizes more seriously than potassium and lithium. In addition, as a selected sample, the distribution of chemical elements of the  $\text{NKL}_x\text{NT}$  ceramics with  $x = 0.074$  sintered at 1000°C is shown in Fig. 3. Although lithium cannot be analyzed by EDS, the homogeneous distribution of sodium, potassium, niobium and tantalum, as shown in Fig. 3, indicates that lithium should be also distributed homogeneously in the ceramic bodies.

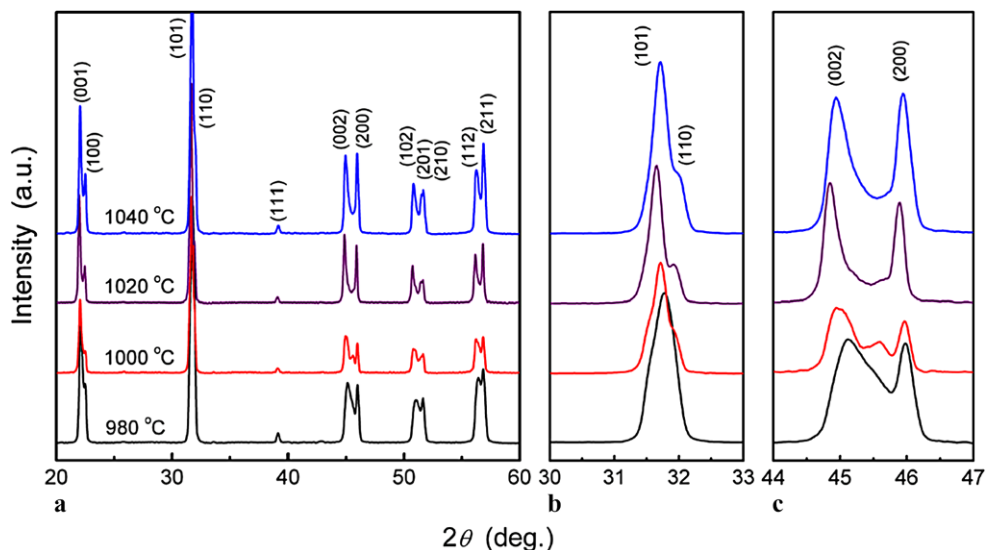
Since the sintering temperature can apparently affect the volatilization of alkali metal ions, and then the phase structure transition behavior, it is achievable for the  $\text{NKL}_x\text{NT}$  ceramics with different Li contents to figure out a corresponding right sintering temperature where the orthorhombic and tetragonal phases can coexist. The phase structure of the  $\text{NKL}_x\text{NT}$  ceramics with various Li contents  $x$  sintered at different temperatures is shown in Table 2. For a given sintering temperature, with increasing Li content  $x$ , the phase structure changes from the orthorhombic to the tetragonal, across a region where the coexistence of the orthorhombic and tetragonal phases occurs. Meanwhile, when the Li content  $x$  is high, the coexistence of the orthorhombic and the tetragonal phases will occur at a relative low sintering temperature.

Picking out the  $\text{NKL}_x\text{NT}$  ceramics with different Li content  $x$  sintered at 1000°C, the lattice parameters were calculated by fitting the XRD profiles, as shown in Fig. 4. The



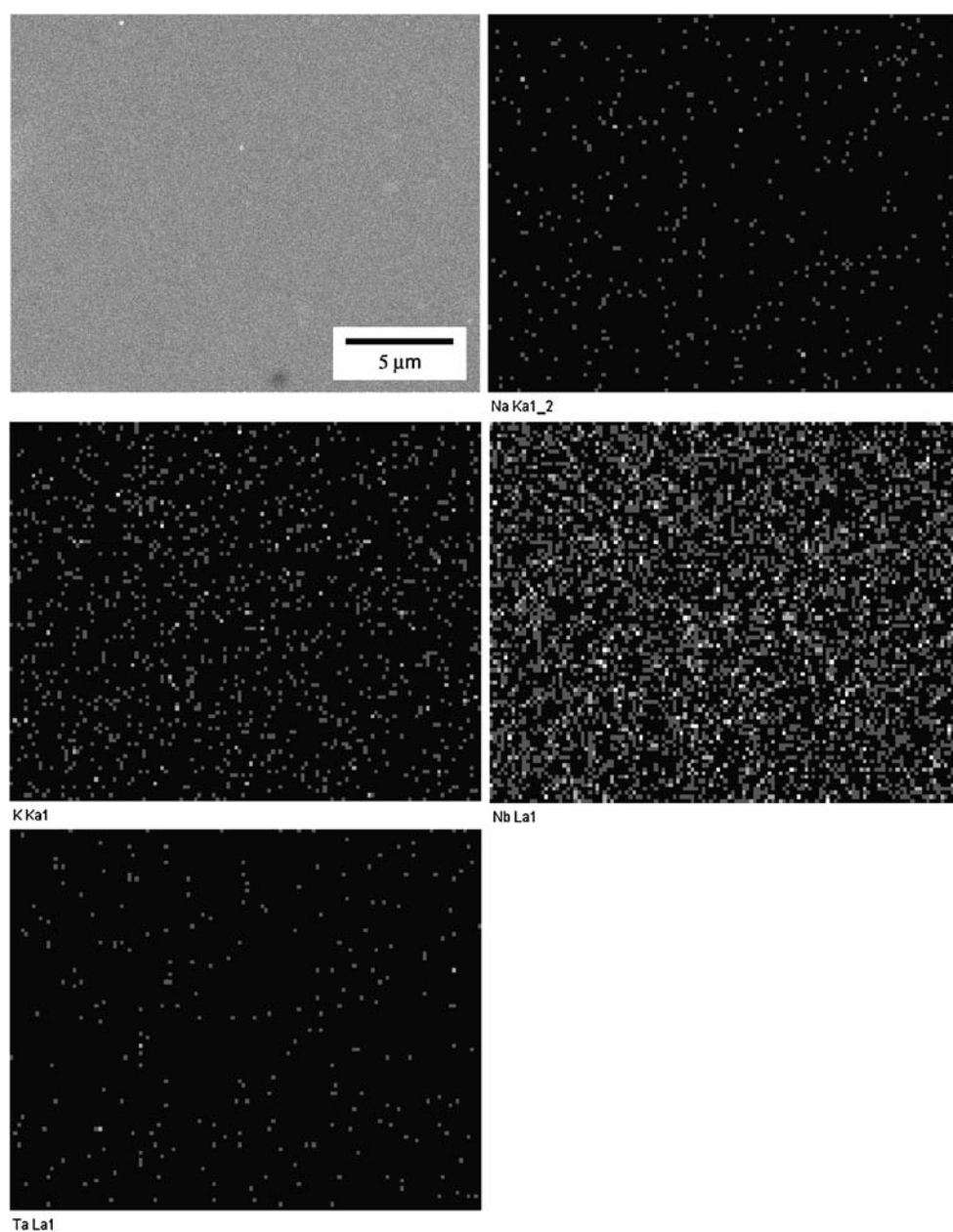
**Fig. 1** Bulk densities of the  $\text{NKL}_x\text{NT}$  ceramics with  $x = 0.042, 0.066, 0.074$  and  $0.090$  sintered at different temperatures

**Fig. 2** X-ray diffraction patterns of the  $\text{NKL}_x\text{NT}$  ceramics with  $x = 0.074$  sintered at 980–1040°C in the ranges of  $2\theta$  **a** from 20° to 60°, **b** from 30° to 33°, and **c** from 44° to 47°



**Table 1** ICP chemical analysis results of Na, K, and Li elements in the  $\text{NKL}_x\text{NT}$  ceramics with  $x = 0.074$  sintered at 980–1060°C

Element	Before sintering	After sintering at different temperatures (°C)				
		980	1000	1020	1040	1060
Na (mg/g)	64.91	64.88	62.67	62.55	60.95	60.73
K (mg/g)	100.069	100.02	99.98	98.98	98.92	99.16
Li (mg/g)	2.927	2.919	2.903	2.894	2.79	2.756

**Fig. 3** Distribution of chemical elements of the  $\text{NKL}_x\text{NT}$  ceramics with  $x = 0.074$  sintered at 1000°C

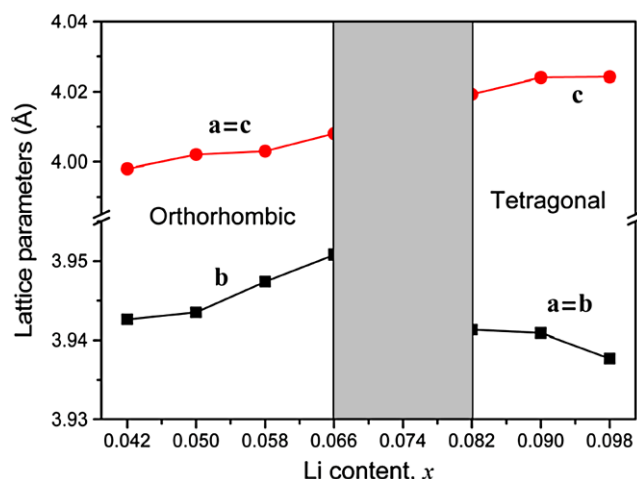
ceramics show the orthorhombic symmetry when  $x \leq 0.066$ , but change to the tetragonal phases when  $x \geq 0.082$ . Apparently, there is a transition zone between the orthorhombic and the tetragonal phases in the range of  $0.066 < x < 0.082$ .

Figure 5 shows the piezoelectric constant  $d_{33}$  and the planar electromechanical coefficient  $k_p$  of the  $\text{NKL}_x\text{NT}$  ceramics sintered at 1000 and 1020°C. As can be seen from Fig. 5,  $d_{33}$  and  $k_p$  show a strong dependence on the Li con-

**Table 2** The phase structure of the  $\text{NKL}_x\text{NT}$  ceramics with various Li contents  $x$  sintered at different temperatures

Sintering temperature (°C)	Li content $x$							
	0.042	0.050	0.058	0.066	0.074	0.082	0.090	0.098
	Phase structure							
980	<i>O</i>	<i>O</i>	<i>O</i>	<i>O</i>	<i>O-T</i>	<i>O-T</i>	<i>T</i>	<i>T</i>
1000	<i>O</i>	<i>O</i>	<i>O</i>	<i>O</i>	<i>O-T</i>	<i>T</i>	<i>T</i>	<i>T</i>
1020	<i>O</i>	<i>O</i>	<i>O</i>	<i>O-T</i>	<i>T</i>	<i>T</i>	<i>T</i>	<i>T</i>
1040	<i>O</i>	<i>O</i>	<i>O-T</i>	<i>T</i>	<i>T</i>	<i>T</i>	<i>T</i>	<i>T</i>
1060	<i>O</i>	<i>O-T</i>	<i>T</i>	<i>T</i>	<i>T</i>	<i>T</i>	<i>T</i>	<i>T</i>

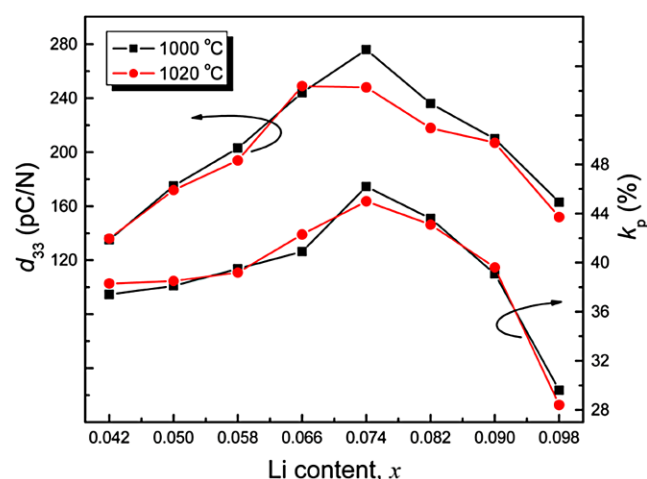
Notes: *O*: Orthorhombic phase, *T*: Tetragonal phase, *O-T*: Coexistence of the orthorhombic and the tetragonal phases



**Fig. 4** Lattice parameters of the  $\text{NKL}_x\text{NT}$  ceramics sintered at 1000°C as a function of Li content  $x$

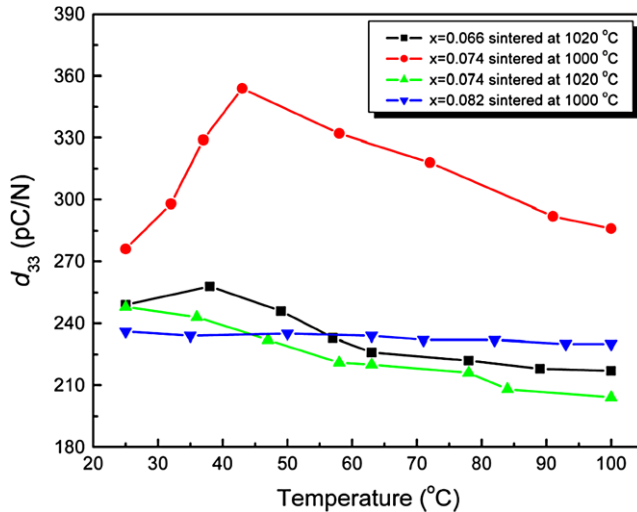
tent  $x$ , and the  $\text{NKL}_x\text{NT}$  ceramics possess relatively good performances in the range of  $0.066 < x < 0.082$ . Moreover, within the same  $x$  range, the sintering temperature can effectively affect the  $d_{33}$  value. For example, the maximum  $d_{33}$  values—249 pC/N and 236 pC/N—are obtained for  $x = 0.066$  sintered at 1020°C and  $x = 0.082$  sintered at 1000°C, respectively. Particularly, through comprehensively optimized effects of Li content and sintering temperature, a maximum  $d_{33}$  value of 276 pC/N was obtained for  $x = 0.074$  sintered at 1000°C, and this value is fairly high for the Li- and Ta-modified NKN ceramics with Sb doping [19]. The highest  $d_{33}$  value should be attributed to the coexistence of the orthorhombic and tetragonal phases near room temperature, as shown in Table 2 and Fig. 4. Relatively similar to the variation behavior of  $d_{33}$ ,  $k_p$  reaches its maximum value of 46.2% for  $x = 0.074$  sintered at 1000°C. In addition, maximum  $k_p$  values—42.3% and 43.6%—are obtained for  $x = 0.066$  sintered at 1020°C and  $x = 0.082$  sintered at 1000°C, respectively.

Figure 6 shows the piezoelectric constant  $d_{33}$  values of several specimens as a function of measuring temperature. For  $x = 0.074$  sintered at 1000°C, the highest  $d_{33}$  value of



**Fig. 5** Piezoelectric constant  $d_{33}$  and planar electromechanical coefficient  $k_p$  of the  $\text{NKL}_x\text{NT}$  ceramics sintered at 1000 and 1020°C

276 pC/N is obtained at room temperature, even though a  $d_{33}$  value of 354 pC/N is obtained when the measuring temperature shifts to 43°C, but it shows a strong temperature dependence from room temperature to 100°C. Moreover, this temperature dependence characterization of  $d_{33}$  value is also observed for ceramics with  $x = 0.066$  and 0.074 sintered at 1020°C. However, for the  $x = 0.082$  composition sintered at 1000°C, in spite of its relatively low  $d_{33}$  value of 236 pC/N as compared with some specimens in this study, exhibits nearly temperature-independent properties from room temperature to 100°C. The  $d_{33}$  value of 236 pC/N is higher than 200 pC/N reported recently by Zhang et al. in  $\text{CaTiO}_3$ -modified  $\text{K}_{0.5}\text{Na}_{0.5}\text{NbO}_3$ -based lead-free ceramics [20], which also exhibits nearly temperature-independent properties. Actually, Zhang et al. obtained a tetragonal phase at room temperature in  $\text{K}_{0.5}\text{Na}_{0.5}\text{NbO}_3$ -based ceramics modified by  $\text{CaTiO}_3$  [20], i.e.,  $T_{o-t}$  shifts downward to below room temperature. From this point of view, we present an easier way to obtain tetragonal phase at room temperature in NKN-based ceramics in the condition of high Li doping amount and low temperature sintering.



**Fig. 6** Temperature dependence of piezoelectric constant  $d_{33}$  of NKL<sub>x</sub>NT ceramics with  $x = 0.066$  sintered at 1020°C,  $x = 0.074$  sintered at 1000 and 1020°C, and  $x = 0.082$  sintered at 1000°C

Figure 7 shows the temperature dependence of dielectric constant of NKL<sub>x</sub>NT ceramics with  $x = 0.058, 0.066, 0.074, 0.082$  and  $0.090$  sintered at 1000°C, the measuring frequency being 100 kHz. As shown in Fig. 7, the temperature dependence of dielectric constant of the NKL<sub>x</sub>NT ceramics shows two phase transitions, i.e., a Curie temperature  $T_c$  and a polymorphic orthorhombic–tetragonal phase transition temperature  $T_{o-t}$ . The corresponding  $T_c$  and  $T_{o-t}$  for  $x = 0.058$  are 425°C and 125°C, respectively. With increasing Li content  $x$ , the  $T_c$  slightly shifts to higher temperatures while  $T_{o-t}$  shifts to lower temperatures. Moreover, the  $T_{o-t}$  shifts downward to below room temperature when the  $x$  value is higher than 0.082, which can be clearly seen by the inset in Fig. 7, and this is in agreement with the analysis results shown in Table 2. For the  $x = 0.082$  composition sintered at 1000°C, due to its  $T_{o-t}$  shifts downward to below room temperature, the  $d_{33}$  value, as shown in Fig. 6, is nearly temperature-independent from room temperature to 100°C. According to the combined results of Figs. 6 and 7, the orthorhombic–tetragonal polymorphic phase transition temperature  $T_{o-t}$  is crucial to affect the property of temperature stability. If the  $T_{o-t}$  shifts downward to near room temperature, it is in favor of obtaining higher piezoelectric constant, but the temperature stability is poor. While the  $T_{o-t}$  shifts downward to a lower than room temperature, a good property of temperature stability can be obtained. The NKL<sub>x</sub>NT ceramics with  $x = 0.082$  possess a good temperature stability and a high  $T_c$  of 445°C, which is a potential Pb-free candidate for the replacement of PZT ceramics.

In order to study the effect of Li content on the ferroelectric properties, the  $P-E$  hysteresis loops of the NKL<sub>x</sub>NT ceramics as a function of  $x$  were measured at room temperature. Figure 8a shows the  $P-E$  hysteresis loops of NKL<sub>x</sub>NT

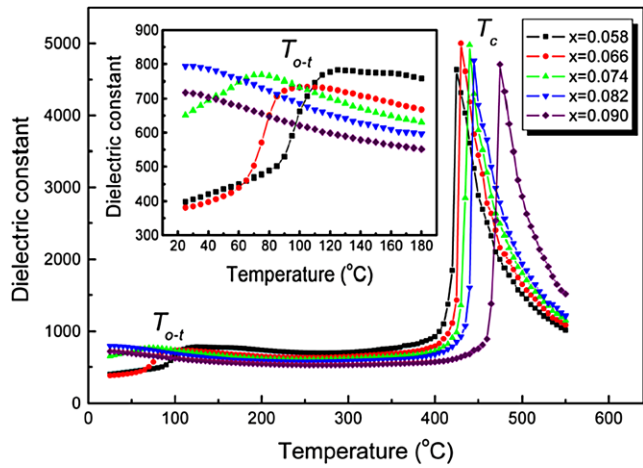


**Fig. 7** Temperature dependence of dielectric constant of NKL<sub>x</sub>NT ceramics with  $x = 0.058, 0.066, 0.074, 0.082$  and  $0.090$  sintered at 1000°C. Measurement was performed at 100 kHz under the heating process. The inset shows an expanded view from room temperature to 180°C

ceramics with  $x = 0.050, 0.058, 0.074, 0.082$ , and  $0.098$  sintered at 1000°C, while the variations of the remnant polarization  $P_r$  and coercive field  $E_c$  with  $x$  are shown in Fig. 8b. A large remnant polarization ( $P_r = 36.6 \mu\text{C}/\text{cm}^2$ ) and low coercive field ( $E_c = 1.47 \text{ kV/mm}$ ) are obtained when Li content  $x$  is 0.050. With increasing Li content  $x$ , the remnant polarization  $P_r$  decreases while coercive field  $E_c$  approximately increases. Meanwhile, as shown in Fig. 8a, when  $x > 0.074$ , although the  $P-E$  loops become non-typical, we consider that these  $P-E$  loops without saturation are different from those with a round shape due to significant current leakage [21]. The present two  $P-E$  loops without saturation should not be induced by the loss derived from leakage currents, because the dielectric loss (at 1 kHz) of all NKL<sub>x</sub>NT ceramics is lower than 0.05. In addition to a strong coercive field obtained in the compositions with  $x > 0.074$ , as shown in Fig. 8b, these  $P-E$  loops without saturation should be attributed to the weakening ferroelectricity of the ceramics induced by high Li content doping. In other words, the decrease in  $P_r$  suggests that increasing  $x$  would weaken the ferroelectricity of the ceramics.

#### 4 Conclusions

Lead-free  $(\text{Na}_{0.535}\text{K}_{0.485})_{1-x}\text{Li}_x(\text{Nb}_{0.942}\text{Ta}_{0.058})\text{O}_3$  piezoelectric ceramics are prepared by the conventional solid-state reaction and normal sintering processes. The combined effects of Li content and sintering temperature on the crystallographic structure, phase transition and electrical properties, were studied. Through modifying composition and optimizing sintering temperature, the room temperature piezoelectric constant  $d_{33}$  is enhanced to 276 pC/N for the ceramics with  $x = 0.074$  sintered at 1000°C, and the  $d_{33}$  value

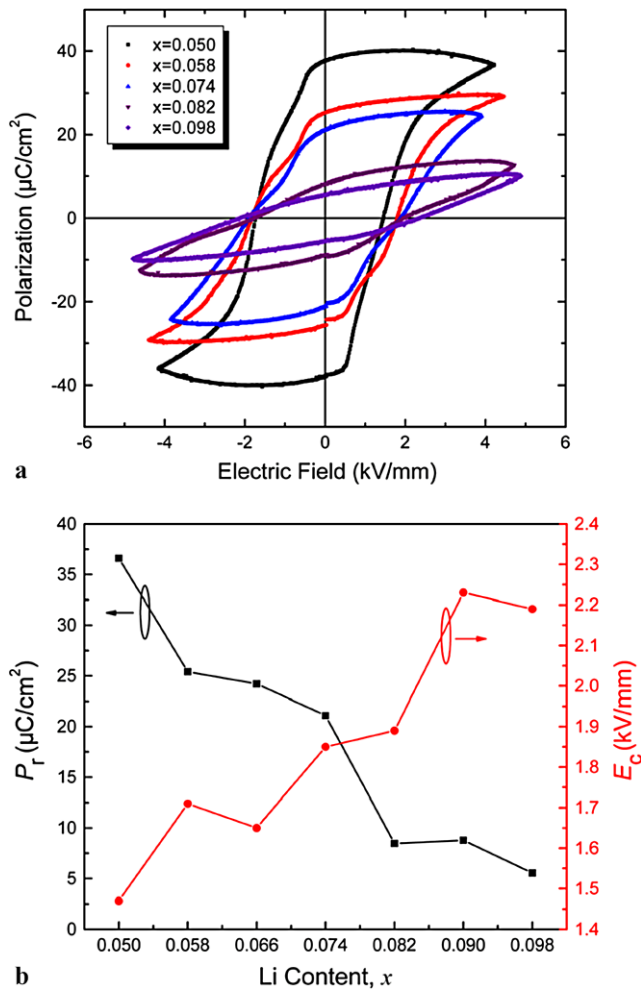


**Fig. 8** **a**  $P$ - $E$  hysteresis loops of  $\text{NKL}_x \text{NT}$  ceramics with  $x = 0.050, 0.058, 0.074, 0.082$  and  $0.098$  sintered at  $1000^\circ\text{C}$ . **b** Remnant polarization and coercive field of the  $\text{NKL}_x \text{NT}$  ceramics sintered at  $1000^\circ\text{C}$  as a function of  $x$

even increases to 354 pC/N when the measuring temperature shifts to 43°C, which is close to its  $T_{o-t}$  temperature. Furthermore, a relatively high piezoelectric constant  $d_{33}$  (236 pC/N), which is nearly temperature-independent

from room temperature to 100°C, is obtained for the ceramics with  $x = 0.082$  sintered at  $1000^\circ\text{C}$  because its  $T_{o-t}$  temperature is moved below room temperature. The present  $\text{NKL}_x \text{NT}$  ceramics with  $x = 0.082$  are considered to be a very promising lead-free piezoelectric material for practical applications because of its low sintering temperature and good piezoelectric property stability.

**Acknowledgements** The authors would like to thank the financial support of Natural Science Foundation of China (Grant Nos. 50772050 and 50621201) and the 973 program (2009CB623304).

## References

1. B. Jaffe, R.S. Roth, S. Marzullo, *J. Appl. Phys.* **25**, 809 (1954)
2. Y. Saito, H. Takao, T. Tani, T. Nonoyama, K. Takatori, T. Homma, T. Nagaya, M. Nakamura, *Nature* **432**, 84 (2004)
3. K. Wang, J.-F. Li, *Appl. Phys. Lett.* **91**, 262902 (2007)
4. N.M. Hagh, B. Jadidian, E. Ashbahian, A. Safari, *IEEE Trans. Ultrason. Ferroelectr. Freq. Control* **55**, 214 (2008)
5. D. Lin, Q. Zheng, C. Xu, K.W. Kwok, *Appl. Phys. A* **93**, 549 (2008)
6. J. Bernard, A. Benčan, T. Rojac, J. Holc, B. Malič, M. Kosec, *J. Am. Ceram. Soc.* **91**, 2409 (2008)
7. D. Lin, K.W. Kwok, H.L.W. Chan, *Appl. Phys. A* **91**, 167 (2008)
8. Y. Dai, X. Zhang, G. Zhou, *Appl. Phys. Lett.* **90**, 262903 (2007)
9. R. Zuo, J. Fu, D. Lv, *J. Am. Ceram. Soc.* **92**, 283 (2009)
10. B. Jaffe, W.R. Cook, H. Jaffe, in *Piezoelectric Ceramics* (Academic Press, New York, 1971), pp. 115–181
11. P. Zhao, B.-P. Zhang, J.-F. Li, *Scr. Mater.* **58**, 429 (2008)
12. Y. Guo, K. Kakimoto, H. Ohsato, *Mater. Lett.* **59**, 241 (2005)
13. Y. Zhen, J.-F. Li, *J. Am. Ceram. Soc.* **89**, 3669 (2006)
14. K. Wang, J.-F. Li, N. Liu, *Appl. Phys. Lett.* **93**, 092904 (2008)
15. M.S. Kim, S.J. Jeong, J.S. Song, *J. Am. Ceram. Soc.* **90**, 3338 (2007)
16. B.M. Jin, I.W. Kim, J.S. Kim, D.S. Lee, C.W. Ahn, J.H. Kwon, J.S. Lee, J.S. Song, S.J. Jeong, *J. Electroceram.* **15**, 119 (2005)
17. Z.Y. Shen, Y. Zhen, K. Wang, J.-F. Li, *J. Am. Ceram. Soc.* (2009). doi:[10.1111/j.1551-2916.2009.03128.x](https://doi.org/10.1111/j.1551-2916.2009.03128.x)
18. P. Zhao, B.-P. Zhang, J.-F. Li, *Appl. Phys. Lett.* **90**, 242909 (2007)
19. J. Wu, T. Peng, Y. Wang, D. Xiao, J. Zhu, Y. Jin, J. Zhu, P. Yu, L. Wu, Y. Jiang, *J. Am. Ceram. Soc.* **91**, 319 (2008)
20. S. Zhang, R. Xia, H. Hao, H. Liu, T.R. Shroud, *Appl. Phys. Lett.* **92**, 152904 (2008)
21. J.F. Scott, *J. Phys., Condens. Matter* **20**, 021001 (2008)